Analysis of geostatistical parameters for texture classification of satellite images

M. Durrieu*, L.A. Ruiz*, A. Balaguer**

**Dept. Cartographic Engineering, Geodesy and Photogrammetry*
***Dept.Applied Mathematics*
Polytechnic University of Valencia (Spain)

(mdurrieu@yahoo.es; laruiz@cgf.upv.es; abalague@mat.upv.es)

Keywords: geostatistics, classification, texture, variogram, satellite images.

Abstract

In this article, we propose and evaluate 23 new geostatistical parameters for texture classification of satellite images. The parameters are computed from the experimental variogram of different subsets of a panchromatic satellite image (QuickBird). The procedure includes an adaptive definition of the window size, as a function of the periodic behaviour of the variogram. Four different methods to compute the variogram are compared, based on the directionality, two of which introduce a pre-classification of the variogram as cyclic or non-cyclic. In the first case, additional parameters are included in the model, in order optimise the final texture classification. The most discriminant features are selected by means of a forward stepwise discriminant analysis. The results show accuracies of up to 81% for a 6 texture classes problem, and over 86% for 5 classes, using between 7 and 9 variables. In future work, the indices will be implemented and evaluated in a pixel by pixel classification procedure.

1. Introduction

Texture analysis for classification of satellite images is usually used when the landscape units are spectrally heterogeneous, as it provides contextual information about the distribution of grey levels around a pixel in the image. Different methods have been attempted in the past to incorporate texture into the classification of digital images. Most techniques used for image texture analysis are based on statistical features, filtering processes or a combination of both. A well known statistical method used in texture analysis is the incorporation of the semivariogram function. As a result, this function gives a curve known as the experimental semivariogram. From this point on, instead of experimental semivariogram, the curve will be called variogram. Miranda et al. (1992, 1998), and Carr and Miranda (1998) started to use information extracted from the variogram to incorporate texture into image classification. Several authors have been using these techniques, introducing new approaches aiming to improve the classification processes. For example, it has been proven that the range is directly related to the size of objects or patterns in an image (Woodcock et al, 1988a, 1988b). On the other hand, the slope at the origin depends on the variability of the objects in the scene (Serra, 1982). Chica-Olmo and Abarca-Hernandez (2000) used the value of the variogram at the first lag for classification, while Maillard (2003) gave more weight to the values of the smaller lags than to those of the greater ones, following a logarithmic scale. Jakomulska and Clarke (2000) applied the variogram to derive a series of indices related to the texture in order to improve the classification results.

In this article, the objective is to design new parameters extracted from the variogram and to evaluate their use for the discrimination of different textures in images. For this purpose, we propose several parameters based on values of the variogram up to the sill, and also the distinction between variograms with cyclic and non-cyclic behaviour, using specific indices for those cases that

are extracted from the first to the second peak of the variogram. However, no attempt to model the variogram is made, due to the necessity of using different models for each type of texture. We base the tests on previous software (Carr, 1996; Pardo-Igúzquiza and Dowd, 2001), which has been modified and adapted for our purposes. Additionally, we introduce new code for the implementation of the new parameters.

2. Materials and Methods

2.1 Area of study and data

The work area is located to the north of the city of Valencia (Spain), and is dominated by agricultural land, especially orange groves and diverse horticulture crops in different stages of their cycle. There are also some residential areas mixed with small forest areas, mainly composed of pine trees. Six types of land cover classes were defined as a basis for testing the potential and utility of the variogram in characterising the texture: orange tree groves, orange tree groves degraded by previous diseases or in early stage of growth, horticulture crops, fallow land, pine trees, and barren soil.

The original image used was a panchromatic QuickBird of the area with a spatial resolution of 0.61 meters. From this image, fifty subsets with a size of 50 rows x 50 columns were obtained for each of the six classes defined, in such a way that each subset contained a portion of scene that was representative of only one of the texture classes considered (Figure 1).

2.2 Calculation of the variogram

Geostatistics studies the autocorrelation of the values of a variable taking into consideration its geographic location. To describe this correlation, it uses the semivariogram, a function that relates semivariance to spatial separation and it provides a concise and unbiased description of the scale and the pattern of spatial variability (P. J. Curran, 1988). For continuous variables, such as reflectance in a given spectral band, the experimental semivariogram is defined as half of the average squared difference between values separated by a given lag, where this lag is a vector in both distance and direction (Atkinson and Lewis, 2000). The experimental semivariogram (here denoted as variogram) is defined as:

$$\gamma(h) = \frac{1}{2N} \sum_{i=1}^{N} \left[Z(x_i) - Z(x_i + h) \right]^2 \quad (1)$$

where $Z(x_i)$ represents the gray level for a generic pixel in the location x_i; N is the number of pixels considered; and h is a vector that represents the distance between pixels in a particular direction.

A variogram can be calculated in the neighbourhood window of each pixel, treating each pixel digital number as the value of a variable, and considering this variable as a realisation of a random spatial process (Chen and Gong, 2004). The distance at which the values of the variable are no longer correlated is defined when the variogram reaches a plateau, and it approximates to the range of the theoretic variogram model. This plateau is known as the sill (Isaaks and Srivastava, 1989). Most of the information is contained in the values of the variogram up to the sill. Variograms often increase continuously with lag distance. However, the variogram is not restricted to such monotonous behaviour and decreasing segments or cyclicity can be observed. Those variogram structures are identified as “hole effect” structures, and can offer valuable information which should not be discarded (Pyrcz and Deutsch, 2003).

For the analyses, FORTRAN code was written to read the image, generate the variograms, and compute the derived parameters to be used in the final classifications.

2.2.1. Determination of the optimal window size

The window size needs to be larger than the range of influence to characterise the first part of the variogram, and large enough to reveal any periodicities in the data (Woodcock et al, 1988a). In this work, these two constraints were considered to be reached using a window size of 30 x 30 pixels. This window size was obtained empirically after trying different sizes and evaluating the results and, consequently, an omnidirectional variogram was derived from a moving window of 30x30 pixels. First, the cyclicity of the omnidirectional variogram is automatically checked. If the variogram is not cyclic, its first maximum value is considered to be very close to the sill of the modeled variogram. For this reason, the distance at which this maximum is reached is assumed to be equivalent to the range of the variogram. Therefore, if there is not cyclicity, the size of the final window is obtained from the value of this denominated experimental range. However, if cyclicity is found, the window size is fixed as the distance to the second maximum.

2.2.2. Variogram computation methods

Four different methods were employed to compute the variogram using the selected window. In each one a modification was introduced:

1) Omnidirectional variogram: It is computed as an average of all possible directions. The first maximum value of the variogram curve is determined, and this distance is considered to be the experimental range. In this method, some indices are calculated with this distance as a limit.

2) Directional variogram: It is calculated over eight different directions: 0°, 22.5°, 45°, 67.5°, 90°, 112.5°, 135° y 157.5°. An angular tolerance of 22.5° to either side of each direction is selected (Figure 2-A). This angular tolerance was chosen with the criteria that there was a sufficient number of data pairs for the calculation of the variogram, and also to keep overlapping between adjacent directions at a minimum. After this, a decision rule is applied in order to determine the direction in which the indices will be computed, basing it on the direction of maximum variability. This is determined as the direction that is orthogonal to the one in which the variogram slope is the smallest. In this method, all the indices proposed up to the first maximum were computed.

3) Cyclic/Non-cyclic directional variogram: The same variogram as in case 2, but applying a new decision rule to distinguish between variograms with cyclic and non-cyclic behaviour. This decision rule is based on the computation of the area between the first two peaks of the variogram. In the cyclic case, the values of the variogram up to the second maximum are included in the calculations, and therefore more indices are obtained.

4) Cyclic/Non-cyclic directional variogram using side angular limits: In this last case the variogram is calculated using the same restrictions in direction and angular tolerance as in the last two cases, incorporating one more limitation: an angular side limit (Figure 2-B). A bandwidth of 3 pixels from each side of every central direction line was selected. Once all of the directions are calculated, the decision rule is applied to determine if the variogram is cyclic or non-cyclic.

2.3 Parameter extraction and selection

To obtain the results of this paper we have used 23 indices, which are based on the variogram values at the first lags up to the two first maximum values. The parameters have been separated into three categories for better understanding. Next, we explain a subset that we determine as representative of each category. In the following mathematical formulas, h_i represents the *ith*-lag and $h = h_{k+1} - h_k, \forall k$; that is, h_i are uniformly separated. $\gamma(h_i)$ is defined by the expression (1).

(1) General parameters. We have computed 8 parameters using the variance of the data representing the gray levels of the digital numbers and considering simple ratios based on $\gamma(h_1)$ (the value of the variogram at the first lag). We also consider different discrete

approximations to the first and the second derivative of the variogram model at the second lag, h_2. For example, we calculate the parameters:

$$Gp1 = \frac{Variance}{\gamma(h_1)};\ Gp3 = \frac{\gamma(h_2)}{\gamma(h_1)};\ Gp4 = \frac{\gamma(h_2)-\gamma(h_1)}{h};\ Gp5 = \frac{\gamma(h_3)-2\gamma(h_2)+\gamma(h_1)}{2h^2}$$

Gp1 and *Gp3* use a ratio with the variogram value in the first lag. *Gp4* approximates the first derivative of the variogram model in h_1 and G*p5* numerically evaluates the second derivative of the variogram model in h_2. Since the variogram tends to reach the sill near the variance, *Gp1* will be an indicator of the relationship between the spatial correlation at short and longer distances. *Gp3* attempts to describe the variability changes at short distances. *Gp4* and *Gp5* show the behaviour of the variogram near the origin and describe the heterogeneity of the objects at short distances in the scene.

(2) First maximum parameters. Eight parameters were calculated in this category, using the variogram values from the first lag up to the first maximum value of the variogram. The lag where $\gamma(h)$ reaches the first maximum, h_{max1}, as well as the average and variance of the considered lags were used. Then, the integral of the variogram was estimated using a composed trapezoidal formula. Some examples are:

$$Fmp1 = h_{\max 1};\ Fmp2 = \frac{1}{\max_1}\sum_{i=1}^{\max 1}\gamma(h_i);\ Fmp3 = \frac{1}{\max_1}\sum_{i=1}^{\max 1}\left(\gamma(h_i)-Fmp2\right)^2;$$

$$Fmp4 = \gamma(h_1)-Fmp2;\ Fmp7 = \frac{h}{2}\left(\gamma(h_1)+2\left(\sum_{i=2}^{\max_1-1}\gamma(h_i)\right)+\gamma(h_{\max_1})\right);$$

Assuming a monotone variogram, *Fmp1* would be defined by the maximum distance in the window. This parameter measures the variability in longer distances. *Fmp2* and *Fmp3* are the mean and the variance, respectively, of all the variogram values between the first value and the value at the first maximum. *Fmp4* is an indicator of homogeneity. *Fmp7* represents the integral of values up to the first maximum.

(3) First to second maximum parameters. A total of 7 additional parameters were derived in the cases where a cyclic variogram is present. In these cases, we considered the variogram values between the first and the second local maximum. We also computed ratios and we numerically evaluated the integral of the variogram from h_{max1} to h_{max2}, which coincide with the lags where the variogram reached the first and second local maximum, respectively. In this category we have defined, for example:

$$Smp1 = h_{\max_2} - h_{\max_1};\ Smp3 = 1-\left(\frac{\gamma(h_{\max_2})}{\gamma(h_{\max_1})}\right);$$

$$Smp5 = \frac{h}{2}\left(\gamma(h_{\max 1})+2\left(\sum_{i=\max_1+1}^{\max_2-1}\gamma(h_i)\right)+\gamma(h_{\max 2})\right);$$

$$Smp7 = 1 - \left[\frac{\frac{h}{2}\left(\gamma\left(h_{\max_1}\right) + 2\left(\sum_{i=\max_1+1}^{\max_2-1} \gamma\left(h_i\right) \right) + \gamma\left(h_{\max_2}\right) \right)}{\frac{h}{2}\left(h_{\max_2} - h_{\max_1}\right)\left(\gamma\left(h_{\max_2}\right) + \gamma\left(h_{\max_2}\right)\right)} \right]$$

Smp1 represents the size of the regularity or structural pattern of a texture. *Smp3* is an indicator of the decay or increase of the variogram cycle, and represents differences in the intensity level of repeated structures. *Smp7* quantifies the "hole effect", and it increases as the variability or contrast of the regularity pattern increases.

Finally, the selection of the most discriminant variables or indices to be used, and the classification of the different textures itself, was done by means of forward stepwise discriminant analysis. In this manner, the best indices were used in each case. In addition a principal component analysis was performed in order to make groups of variables depending upon the type of information that they provide.

3. Results

The principal components analysis is useful for grouping variables that explain the same properties in a multivariate problem. Two different analyses were done, one using the set of indices that considers only values up to the first maximum, and a second one using the set of indices with values up to the second maximum, that were conceived to provide information only about the cyclic variograms, this is, those that represent textures with a periodic or semi-periodic pattern. In both cases, several well defined groups of variables are noticeable. Interpreting those groups, we find that in the first case they include indices that represent properties such as spatial frequency, gray level variability, contrast or homogeneity. For the cyclic variables, they are grouped according to the presence of regular structures in the landscape, irregular patterns ("dampening" effect or decay of the variogram), or even the magnitude of the "hole effect".

In the application of the forward stepwise discriminant analysis for the selection of variables to be included in the classification process, depending on the method used to compute the variogram, between 7 and 9 variables in the model were usually sufficient to obtain satisfactory results. In addition, it was observed that at least one variable belonging to each of the former semantic groups of variables, interpreted in the principal component analysis planes, was included. They were not always the same variables, but they represented the same group of texture properties.

Since the two land cover classes corresponding to orange groves were those that generated more confusion in all cases, an additional second analysis was undertaken where these two classes were combined into one. As a result, the accuracy increased in all cases. Regarding the different methods used to compute the variogram, the best overall accuracy in the classification was obtained using the *cyclic/non-cyclic directional variogram with side angular limits*: 81% in a problem of six texture classes, and 86.7% considering only five classes (Tables 1 and 2). However, the use of the *onmidirectional variogram* produced similar results, 77.7% and 85.7%, respectively, while the lowest accuracy corresponded to the *directional variogram*.

Studying the producer and user accuracies, it was observed that the *omnidirectional variogram* perform better in the uniform and homogeneous textures, such as barren soil and fallow fields, but the *cyclic/non-cyclic directional variogram with side angular limits* provides higher accuracy values in those textures containing a gray level pattern with spatial structure, like the textures of orange groves. Therefore, the classes with a marked directionality were benefited with the incorporation of the directional and cyclic restriction in the analysis. However, for those classes having intermediate properties, the results are not so evident.

Finally, the most discriminant parameters were those that included the first value of the variogram in their formulas, for instance, the ratio of the first and second values of the variogram, or the subtraction of the first value by the average of all the values up to the first maximum. Other variables that provided good results were: the average of all the values up to the first maximum, and the distance at which the first maximum value was reached (similar to the range).

4. Conclusions

An exhaustive number of indices extracted from the variogram of different texture images has been proposed in order to classify the images according to their type of texture. The results show that, due to the correlation between indices, they can be grouped in approximately nine sets of indices, each of which would explain a different texture property. In this manner, the information inherent to the variogram can be parameterised and then used for texture classification.

The method proposed for the definition of an adaptive window size, based on the computation of the first and second maximum values for every neighbourhood, seems to perform properly.

The new approach based on the distinction of cyclic and non-cyclic variograms, and the computation of a directional variogram with side angular limits, allows us to discriminate more accurately those textures that present a directionality, or at least a certain pattern or spatial structure, such as orange groves or linear crops. However, the omnidirectional variogram performs better for more uniform and homogeneous textures.

Among the indices or parameters with higher discrimination power are those that include the first value of the variogram. On the other hand, the parameters obtained from the first to the second maximum offer specific information about the periodicity in the image, and as such are only considered when the variograms are cyclic. The classification results are very encouraging, especially taking into consideration that the original data is a panchromatic image with only one band. Future work will be focused on the implementation of a selection of the proposed indices to achieve the classification of images on a pixel by pixel basis.

Acknowledgements.

This research was supported by the Spanish Ministry of Science and Technology and the FEDER, in the frame of the projects BTE2002-04552 and REN2003-04998.

5. References

- Abarca-Hernández, F., Chica-Olmo, M., 1999. Evaluation of geostatistical measures of radiometric spatial variability for lithologic discrimination in Landsat TM images. Photogrammetric Engineering & Remote Sensing, 65 (6), 705-711.
- Atkinson, P.M., Lewis, P. 2000. Geostatistical classification for remote sensing: an introduction. Computers & Geosciences 26, 361-371.
- Carr, J.R., 1996. Spectral and textural classification of single and multiple band digital images. Computers & Geosciences, 22 (8), 849-865.
- Carr, J.R., Miranda, F.P., 1998. The semivariogram in comparison to the co-occurrence matrix for classification of image texture. IEEE Transactions on Geoscience and Remote Sensing, 36 (6), 1945-1952.
- Chica-Olmo, M., Abarca-Hernández, F., 2000. Computing geostatistical image texture for remotely sensed data classification. Computers & Geosciences, 26, 373-383.
- Curran, P.J., 1988. The semivariogram in remote sensing: an introduction. Remote Sensing of Environment, 24, 493-507.

- Curran, P.J., 2001. Remote sensing: using the spatial domain. Environmental and Ecological Statistics, 8, 331-344.
- Isaaks, E.H., Srivastava, R.M., 1989. Applied Geostatistics. Oxford, Oxford University Press.
- Jakomulska, A., Clarke, K.C., 2000. Variogram-derived measures of textural image classification, application to large scale vegetation mapping. geoENV III – Geostatistics for Environmental Applications, 345-355. November 22-24, 2000.
- Maillar, P., 2003. Comparing texture analysis methods through classification. Photogrammetric Engineering & Remote Sensing, 69 (4), 357-367.
- Miranda, F.P., MacDonald, J.A., Carr, J.R., 1992. Application of the semivariogram textural classifier (STC) for vegetation discrimination using SIR-B data of Borneo. International Journal of Remote Sensing, 13 (12), 2349-2354.
- Miranda, F.P., Fonseca, L.E.N., Carr, J.R., 1998. Semivariogram textural classification of JERS-1 (Fuyo-1) SAR data obtained over a flooded area of the Amazon rainforest. International Journal of Remote Sensing, 19 (3), 549-556.
- Pardo-Igúzquiza, E., Dowd, P.A., 2001. VARIOG2D: a computer program for estimating the semi-variogram and its uncertainty. Computers & Geosciences, 27, 549-561.
- Pyrcz, M. J., Deutsch, C. V., 2003. The whole story on the hole effect. Searston, S. (ed) Geostatistical Association of Australasia, Newsletter 18, May 2003.
- Serra, J., 1982. Image analysis and mathematical morphology. Academic, New York.
- Woodcock, C.E., Strahler, A.H., Jupp, D.L.B., 1998a. The use of variograms in remote sensing I: Scene models and simulated images. Remote Sensing of Environment, 25 (3), 323-348.
- Woodcock, C.E., Strahler, A.H., Jupp, D.L.B., 1998b. The use of variograms in remote sensing II: real digital images.

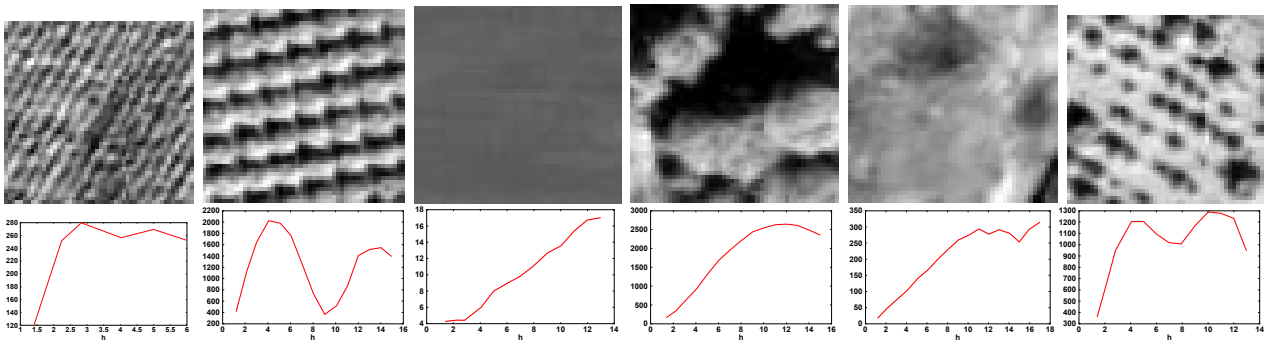

a) b) c) d) e) f)

Figure 1. Examples of texture class images and their respective variograms. a) horticulture crops; b) orange groves; c) fallow fields; d) pine trees; e) barren soil; and f) degraded orange groves.

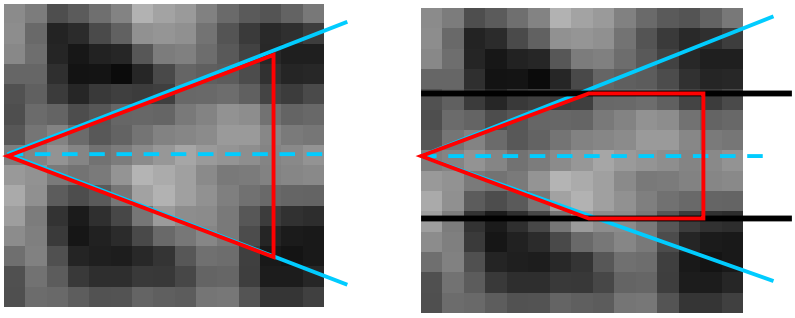

a) b)

Figure 2. Schematic description of the differences between (a) the *directional variogram*, and (b) the *directional variogram using side angular limits*. The blue dashed line represents the direction of the variogram. The angle between the two blue continuous lines is the angular tolerance. The two black lines are the side limits, and the pixels inside the red figures are those used for the computation of the variograms.

	Omnidirectional Variogram		Directional Variogram		Cyclic/Non-Cyclic		Cyclic/Non-Cyclic + limits	
	Producers accuracy	Users accuracy	Producers accuracy	Users accuracy	Producers accuracy	Users accuracy	Producers accuracy	Users accuracy
Crops	80,0	97,6	86,0	81,1	80,0	95,2	**86,0**	82,7
Barren soil	**82,0**	77,4	72,0	66,7	76,0	65,5	78,0	72,2
Orange groves	62,0	70,5	64,0	71,1	**86,0**	81,1	78,0	84,8
Fallow fields	**94,0**	83,9	82,0	75,9	84,0	75,0	78,0	79,6
Pine trees	**94,0**	82,5	82,0	83,7	78,0	90,7	88,0	95,7
Deg. Orange groves	54,0	55,1	52,0	57,8	70,0	72,9	**78,0**	73,6
Overall	**77,7**		**73,0**		**79,0**		**81,0**	

Table 1. Comparison of accuracies obtained with the four different methods for a texture classification problem of six classes.

	Omnidirectional Variogram		Directional Variogram		Cyclic/Non-Cyclic		Cyclic/Non-Cyclic + limits	
	Producers accuracy	Users accuracy	Producers accuracy	Users accuracy	Producers accuracy	Users accuracy	Producers accuracy	Users accuracy
Crops	80,0	95,2	86,0	75,4	82,0	82,0	**86,0**	78,2
Barren soil	**82,0**	73,2	72,0	66,7	72,0	66,7	74,0	75,5
Orange groves	83,0	100,0	82,0	98,8	92,0	97,9	**93,0**	97,9
Fallow fields	**90,0**	83,3	82,0	75,9	86,0	74,1	82,0	78,8
Pine trees	**96,0**	73,8	86,0	82,7	80,0	90,9	92,0	93,9
Overall	**85,7**		**81,7**		**84,0**		**86,7**	

Table 2. Comparison of accuracies obtained with the four different methods for a texture classification problem of five classes.